Correlation between acoustic emission signals and friction behavior under different sliding configurations and materials pairs

Malik Yahiaoui, Jean-Yves Paris, Jean Denape

Correlation between acoustic emission signals and friction behavior under different sliding configurations and materials pairs

M. Yahiaoui[1, a], J-Y. Paris[1, b] and J. Denape[1, c]

[1] Université de Toulouse; INPT-ENIT; LGP (Laboratoire Génie de Production), 47 avenue d'Azereix, B.P. 1629, 65016 Tarbes, France

[a]malik.yahiaoui@enit.fr, [b]jean-yves.paris@enit.fr, [c]jean.denape@enit.fr

Keywords: Acoustic emission, friction, contact temperature, wear, speed camera, tungsten carbide, alumina, thermoplastic polyurethane.

Abstract. This work focuses on the acoustic emission signals related to three different tribological systems: a rotary sliding contact between WC-Co pins against alumina flat counterfaces, a fretting contact between alumina pins against alumina flat counterfaces and a reciprocating sliding flat on flat contact between thermoplastic polyurethanes (TPU) and a steel counterface. This document relates dependences observed between tribological behaviors and variations of acoustic emission signals. Therefore, a third body approach is used to explain these correlations and to highlight the aspect of nature and associated energy of acoustic emission sources.

Introduction

Tribological systems are studied using acquisition systems associated to several kinds of sensors. For example, load and torque sensors are performed to measure the friction coefficient, thermocouples to evaluate the contact temperature, vision systems to follow the evolution of the contact morphology, etc. However, the optical observation of the active surfaces during sliding friction is impossible in most of the tribological systems. In this way, the study of acoustic emission (AE) signals emitted by the closed sliding contact is an interesting solution.

Acoustic emission defines mechanical waves produced by the release of elastic stress energy from a localized source. Baranov et al. [1] identified different sources of acoustic emissions (e.g. cracks propagation and debris formation) and their associated range of energy and of frequency (e.g. 106 to 108 aJ for the microcracks formation) in the sliding contacts. They also specified a list of material physicochemical and mechanical properties and friction conditions influencing the acoustic emission amplitude. For example, a rough relief, a high hardness and an abrasive wear are factors of increase in amplitude. Conversely, fine grains, slow sliding velocity and adhesive wear are factors of decreasing amplitude of the acoustic emission signals.

This work focuses on the acoustic emission signals related to three different tribological systems:

- A rotary sliding contact between a WC-Co pin against an alumina flat counterface [2];
- A reciprocating sliding flat on flat contact between a thermoplastic polyurethane (TPU) and a steel counterface [3];
- A fretting contact between an alumina pin against alumina flat counterface [4].

This study gathers several test campaigns dealing with effects of contact parameters, as load and velocity, on acoustic emission. Moreover, the studied contacts highlighted the dependence of acoustic emission signals towards material physicochemical properties in relation to the contact thermomechanical responses. More generally, these experiments showed the links that can be revealed between the overall tribological system consideration and the acoustic emission.

Acoustic Emission Device

Acquisition Setup. Acoustic emission acquisitions are performed using a filter of vibrational phenomena which are unrelated to friction (e.g. movement of mechanical parts of the tribometer).

Hence, before each experiment, a threshold of mechanical noises must be set. In addition, the large band piezoelectric sensors (references Micro-80 and Pico of the company Euro Physical Acoustics) used in this study have an optimum sensibility between ultrasonic frequencies of 0.1 MHz and 1 MHz.
The sensor fixation near the sliding contact is a crucial step in the acquisition setup called the coupling. This coupling was performed by a water-based adhesive containing styrene acrylic co-polymer. This adhesive allows a good transmission of acoustic signals, dries in few seconds and the sensors are easily detached after the experiments. Hsu-Nielsen sources were created to test the coupling quality (standard NF EN 1330). This procedure consists in the breaking of standard pencil leads (hardness 2H and 0.5 mm in diameter) near the future sliding zone. The Hsu-Nielsen sources generate repeatable acoustic emission signals (i.e. standard hits). Finally, the coupling is achieved when the acoustic signal transmission leads to acquisition amplitude over 90 dB and ideally 100 dB.

Signals Processing. The recorded acoustic emission signals need to be pre-processed to avoid a too high storage of data and laborious post-processing operations. Therefore, the signals are not continuously recorded but are cut in hits. These hits correspond to events generating acoustic emission signals in the contact with amplitudes overpassing the fixed threshold. This threshold depends on the noise created by the mechanical parts surrounding the contact. The signals coming from the sensor are also pre-amplified before being treated by the acquisition card of the computer.
A moving window of acquisition needs to be defined to obtain entire hits waveform without missing a part of them or to avoid echoes. This window is characterized by the parameters of sample rate, pre-trigger, peak definition time (PDT), hit definition time (HDT) and hit lockout time (HLT). These parameters depend on the tribological system and on the propagation of the acoustic emissions in the considered materials.
In this study, only the energy of the acoustic emission signals is considered. More particularly, the absolute energy E_a is calculated by the integration of the squared signal $s(t)$, translation of the mechanical pulses in electrical tension, over the period of a hit and normalized by the resistance Re of the acoustic emission device (Eq. 1).

$$E_a = \frac{1}{R_e}\int_T s^2(t)\cdot dt \tag{1}$$

Experimental Procedures

WC-Co / Alumina Sliding Contact. The wear mechanisms of cemented carbide samples were studied at the LGP laboratory with a rotary tribometer (Fig. 1a). During experiments, a pin-on-disk contact is realized. The samples have a spherical tip with a radius of 4.37 mm and slides against a flat alumina counterface. The wear of these samples was carried out at various normal loads FN between 0 and 300 N with velocities v between 0.1 and 1 m·s-1 with a test time t of one hour. Nominal conditions were also set at 264 N and 0.5 m·s-1 always during one hour. The normal load and the torque were measured to calculate the friction coefficient μ. The acoustic emission sensor was coupled on the upper shaft at 120 mm from the fixed insert to obtain optimum signals without saturation (Fig. 1b).

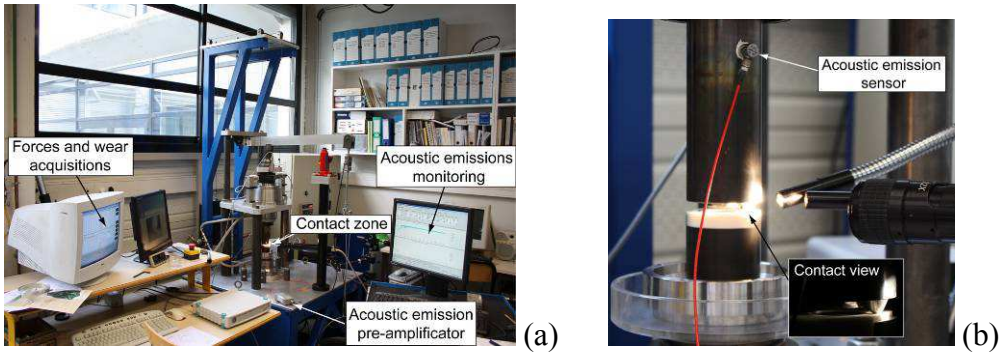

Fig. 1: Rotary tribometer and AE device configuration (LGP laboratory): a - general view of the rotary tribometer; b - view of the Micro-80 sensor coupled near the contact.

Three different WC-Co samples were considered with the references P8, P12 and P16 from the company Varel Europe. These references respectively correspond to cobalt contents of 8 ± 1, 12 ± 2 and 15 ± 1 wt.%. In addition, others physicochemical and mechanical parameters have been measured for these samples (Table 1). Simply, as indicated by the cemented carbide manufacturers, when the cobalt content or the WC grains size increases, the hardness decreases and the fracture toughness increases.

Table 1: Physicochemical and mechanical properties of WC-Co samples P8, P12 and P16.

WC-Co samples	P8	P12	P16
Cobalt content [wt. %]	8 ± 1	12 ± 2	15 ± 1
Mean grain size [µm]	3 ± 0.1	7 ± 3	5 ± 1
Hardness [HV 2 kg/10 s]	1326 ± 31	1095 ± 29	1061 ± 3
Fracture toughness [MPa·m1/2]	11.0 ± 0.4	19.5 ± 0.8	18.2 ± 0.2

TPU / Steel Reciprocating Sliding Contact. Wear experiments on TPU against a steel counterface were performed on a reciprocating long stroke tribometer at the ITA laboratory (Zaragoza, Spain) (Fig. 2). The selected TPU material has a density of 1.23 ± 0.02 g·cm^{-3}, a non-significant mineral charge content of 0.05 wt.% and an hardness of 54 ± 1 Sh(D). A flat-on-flat contact was set between a rectangular TPU sample (25 mm × 15 mm × 10 mm) and a steel countermaterial (2000 mm × 37 mm × 9 mm). Three experimental campaigns were carried out to study the effects of load (from 166 N to 401 N), velocity (at 0.32 m·s^{-1} and 0.5 m·s^{-1}) and temperature (from 21 °C to 75 °C) to establish the TPU material tribological behavior against a heated steel counterface. The Pico EA sensor was fixed near the contact on the mobile part.

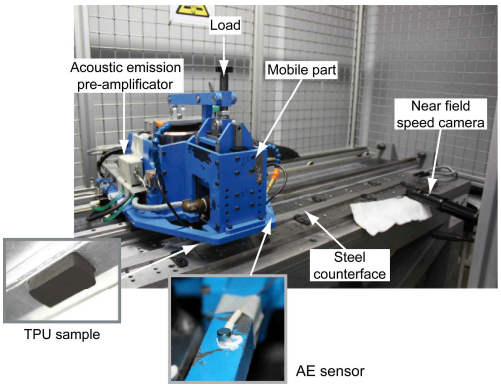

Fig. 2: Reciprocating long stoke tribometer and AE device configuration (ITA laboratory).

Alumina / Alumina Fretting Contact. Friction experiments of alumina pins against a flat pure alumina were carried out with a fretting device at the LGP laboratory (Fig. 3). The alumina pins are hemispherical with a radius of 20 mm. The experiments were performed with progressive normal loads F_N form 6 N with a step of 2 N each 5 min. A tangential force F_T is generated by an inputted driving force. This force oscillates between -20 and 20 N (± 1 N).

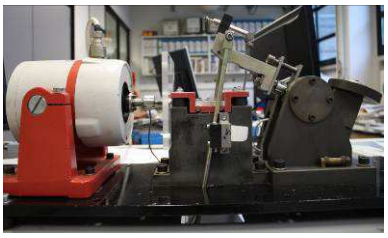
(a)

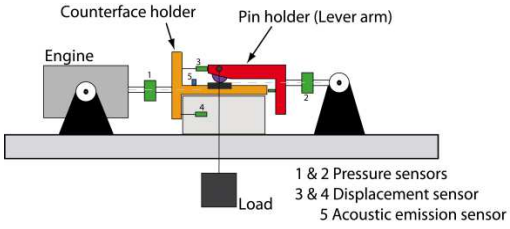

(b)

Fig. 3: Fretting device configuration and AE device configuration (at the LGP laboratory): a – photography of the device; b – detailed sketch of the device.

The pins of alumina at 99.7 % were manufactured by sintering under pressure and referenced as A99. The counterfaces of alumina at 99.7 % were realized by spark plasma sintering (SPS) and referenced A99S. The SPS process acts by significantly reducing the alumina mean grains size (Table 2). This process also enhances the mechanical properties of the alumina.

Table 2: Physical and mechanical properties of alumina materials (CIRIMAT laboratory data [4]).

Alumina samples	A99	A99S
Density [g·cm^{-3}]	3.92 ± 0.05	3.98 ± 0.05
Mean grain size [µm]	8 ± 0.2	2.5 ± 0.2
Hardness [HV 1 kg/10 s]	1570 ± 70	2010 ± 110
Ultimate strength [MPa]	320 ± 5	650 ± 10
Fracture toughness [MPa·m$^{1/2}$]	5 ± 0.1	5 ± 0.2

AE Device Parameters. The wear experiments with the WC-Co samples generated intense acoustic emission signals and the threshold was then set at 40 dB with the lowest pre-amplification of 20 dB (Table 3). The other parameters (e.g. PDT and HLT) were selected in order to obtain the shortest but complete hits wave form. For the other experiments, the threshold and the pre-amplification were respectively set at 30 dB and 40 dB.

Table 3: Acoustic emission acquisition parameters of the various tribometer.

AE parameters	Rotary tribometer	Reciprocating long stoke tribometer	Fretting tribometer
Threshold [dB]	40	35	27
Pre-amplification [dB]	20	40	40
Sample rate [kHz]	5000	1000	5000
Pre-trigger [µs]	50	256	50
PDT [µs]	1000	200	200
HDT [µs]	2000	800	500
HLT [µs]	20000	1000	1000

Results and Correlations

AE and Mechanical Energy. For all the configurations, the amount of mechanical energy W transmitted through the sliding contact is equal to the product of the transverse force F_T by the travel distance L or by the velocity v multiplied by the time t (Eq. 2).

$$W = F_T \cdot L = F_T \cdot v \cdot t \quad (2)$$

Most of this energy is converted to heat during friction and only a small part is transformed in elastic waves. In this way, the energy E_a of the acoustic emission signals should increase with the overall mechanical energy W. This dependence clearly appears in the experiments studied here:

- For example, on the rotary tribometer with the WC-Co samples, E_a globally increases from 0 to $7 \cdot 10^{10}$ aJ when the sliding velocity increases from 0.1 to 1 $m \cdot s^{-1}$ and *vice versa* (Fig. 4a);
- During fretting experiments at progressive load with the alumina A99S, the work W decreases with time meanly because of a reduction of the stroke and the travel distance (Fig. 4b) and so as the absolute energy E_a;
- With the reciprocating tribometer and the TPU samples, the work is approximately constant as a result of the imposed travel distance and the slightly increasing friction force. Again, the absolute energy E_a follows the variation of the overall mechanical energy W (Fig. 4c).

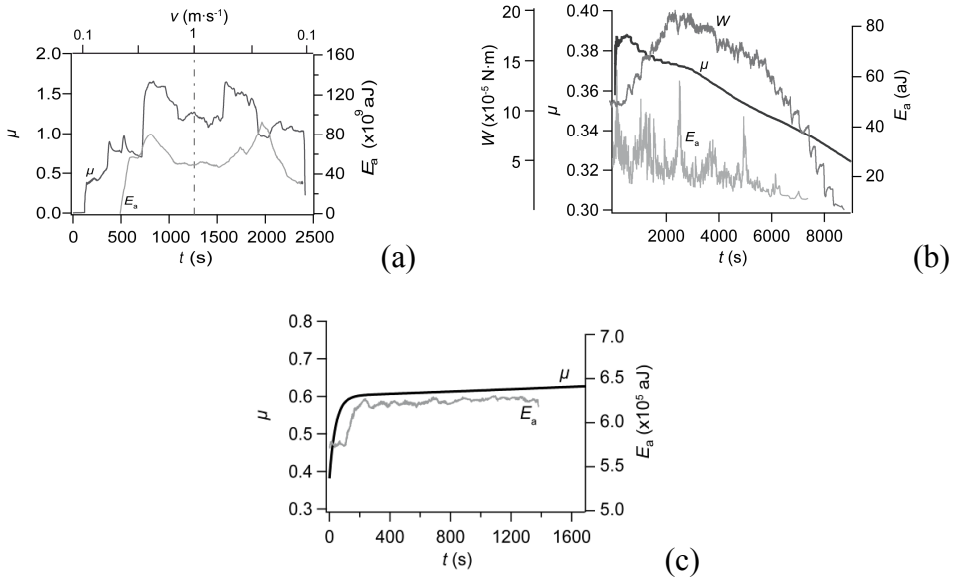

Fig. 4: Work, Friction coefficient and absolute energy results: a - experiment at progressive velocities (from 0.1 to 1 $m \cdot s^{-1}$ and from 1 to 0.1 $m \cdot s^{-1}$) on the rotary tribometer with the P8 WC-Co sample; b - fretting experiments at progressive load (from 6 to 48 N) with A99S counterface; c - results at constant a load of 248 N on the reciprocating tribometer with a TPU sample.

More precisely, the absolute energy E_a tends to follow the friction coefficient changes. Indeed, even with a non-linear evolution of the friction coefficient, the acoustic absolute energy exhibits the same variations (Fig. 4a). These observations indicate an affine relationship between the friction and the acoustic emission energy.

Effect of Material Properties. Even if the energy E_a follows the friction coefficient changes, its amplitude depends on the nature of the AE sources. In this way, the mean friction coefficient of the WC-Co samples decreases with the cobalt content (*i.e.* in order from P8, P12 to P16) but the AE absolute energy appears to be the highest on average for the P12 (Fig. 5).

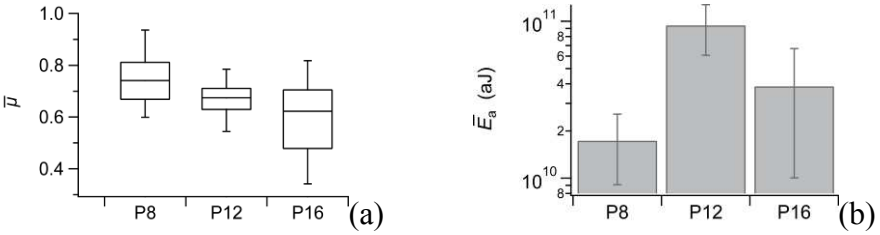

Fig. 5: Results of experiments with the WC-Co samples at constant load of 264 N over three repeatability tests: a - average of friction coefficients (box and whiskers chart); b - average of absolute energy.

Observations of the P12 samples worn surfaces display a great proportion of transgranular cracks. Further study on these cemented carbides showed that the transgranular cracking mode was associated to the P12 sample coarse WC grains. The P8 and P16 samples, with finer microstructures, show predominantly intergranular cracks during wear. This difference of crack mode explains that the P12 sample generates more energetic acoustic emission signals. Indeed, the energy dissipation induces by transgranular crack propagation is greater than the one induces by intergranular mechanism. This observation is also reflected by the fracture toughness K_{IC} measured on the samples (Table 1).

Another example of the influence of materials and the importance of the nature of AE sources is brought by the experiments on the TPU polymer. During these experiments, it was shown that a stick-slip phenomenon appear in the contact after a threshold of load (around 270 N). The stick-slip produces a higher discrepancy on forces but friction meanly verifies an Amontons-Coulomb law (Fig. 6a). Concerning the absolute energy, before this threshold, E_a increases because increasing load generates a higher mechanical energy in the contact (Fig. 6b). After this threshold, the stick-slip mechanisms modify the nature of the AE sources by a change of sliding mode in the contact and a drop of absolute energy is then observed.

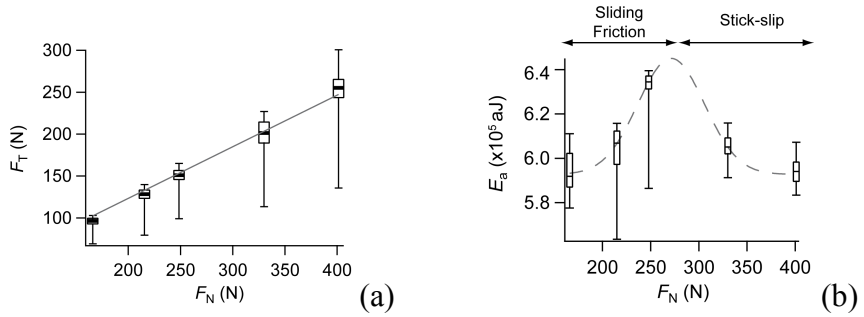

Fig. 6: Effect of the stick-slip phenomenon: a – Amontons-Coulomb law tangential force *vs.* normal force; b – absolute energy *vs*. normal force.

Discussions

Tribological behaviors can be described using a third body approach by considering the speed accommodation mechanisms in the contact [5, 6]. In this way, acoustic emission sources can be localized at the accommodation sites S_i and their nature can be associated to an accommodation mode M_j (Fig. 7).

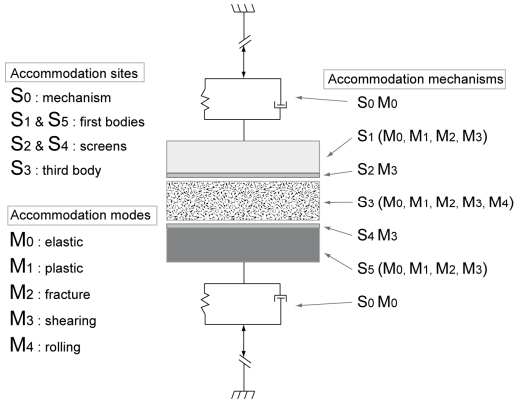

Fig. 7: Mechanisms of speed accommodation in the tribological system (after [6]).

With this approach, friction depends on the accommodation mechanisms acting at the interface through the third body. A poor third body action could provoke more direct interactions of the first bodies and more energetic modes (*i.e.* elastic, plastic and fracture) located on the samples surface. An active third body separates the first bodies and implies low energetic modes (i.e. shearing and rolling) inside the third body itself. Accordingly, the increase of the friction coefficient is associated to the increase of sites density and then of acoustic emission sources density. However, the amount of energy dissipated by these sources depends on the mode of accommodation.
For example, concerning the stick-slip mechanism for the TPU/steel contact, the drop of acoustic emission energy can be related to less energetic mechanisms occurring during the stick periods. Indeed, during stick periods, the TPU polymer is elastically or plastically deformed (S_1M_0 or S_1M_1). Otherwise, during slip periods, the TPU slides against the steel counterpart, it wears (S_1M_2) and rolls are formed (S_1M_4). In addition, the third body shears (S_3M_3) and rolling accommodations (S_3M_4) are performed at the interface.

Conclusion

Three experimental devices were studied here: a rotary tribometer with a WC-Co / alumina contact, a reciprocating tribometer with a TPU / steel contact and a fretting tribometer with a alumina / alumina contact. In one hand, these experiments showed that the calculated acoustic emission energy follows the friction coefficient changes. In other hand, they also point out that material properties affect the level of energy of the acoustic emission signals. Eventually, a third body approach gathers these aspects. The friction coefficient and acoustic emission signals are related by the accommodation sites activated during friction. The acoustic emission energy dissipated by the sliding contact is function of the nature of acoustic emission sources associated to the modes of accommodation.

References

[1] V. Baranov, E. Kudryavtsev, G. Sarycgev and V. Schavelin. Acoustic emission in friction. Elsevier, 2007.

[2] M. Yahiaoui, Comportement tribologique de diamants polycristallins et de carbures cémentés WC-Co avec traitements de graduation - application aux inserts et taillants d'outils pour le forage de formations rocheuses fortement abrasives, Ph.D. thesis, Université de Toulouse (2013).

[3] F. J. Martínez, M. Canales, N. Alcalá, M. A Jiménez, M. Yahiaoui, A. G. Ural, J.-Y. Paris, K. Delbé and J. Denape, Analysis of wear mechanism in TPU-steel contact pair by means of long stroke tribometer tests, in: Proceeding of LUBMAT 2012.

[4] A. G. Ural, Performances en frottement de composites alumine-métal avec ou sans nanotubes de carbone : identification des conditions de grippage et des mécanismes d'usure, Ph.D. thesis, Université de Toulouse (2011).

[5] Y. Berthier. Maurice Godet's Third Body. In D. Dowson, C.M. Taylor, T.H.C. Childs, G. Dalmaz, Y. Berthier, L. Flamand, J.-M. Georges and A.A. Lubrecht, editeurs, The third body concept interpretation of tribological phenomena, volume 31 of Tribology Series, pages 21–30. Elsevier, 1996.

[6] J. Denape, Y. Berthier and L. Vincent. Fundamentals of tribology and bridging the gap between the macro- and micro/nanoscales, chapitre Wear particle life in sliding contact under dry conditions: third body approach, pages 393–411. Kluwer Academic Publishers, 2001.